Large Variations in Southern Hemisphere Biomass Burning During the Last 650 Years

Z. Wang, *et al.*

Science **330**, 1663 (2010);
DOI: 10.1126/science.1197257

4. Z. H. Dughaish, *Physica B* **322**, 205 (2002).
5. H. Lin, E. S. Bozin, S. J. L. Billinge, E. Quarez, M. G. Kanatzidis, *Phys. Rev. B* **72**, 174113 (2005).
6. U. V. Waghmare, N. A. Spaldin, H. C. Kandpal, R. Seshadri, *Phys. Rev. B* **67**, 125111 (2003).
7. J. M. An, A. Subedi, D. J. Singh, *Solid State Commun.* **148**, 417 (2008).
8. J. R. Sootsman *et al.*, *Angew. Chem. Int. Ed.* **47**, 8618 (2008).
9. T. Egami, S. J. L. Billinge, *Underneath the Bragg Peaks: Structural Analysis of Complex Materials* (Pergamon Press, Elsevier, Oxford, England, 2003).
10. S. J. L. Billinge, I. Levin, *Science* **316**, 561 (2007).
11. Materials and methods are available as supporting material on *Science* Online.
12. B. E. Warren, *X-ray Diffraction* (Dover, New York, 1990).
13. I.-K. Jeong, T. Proffen, F. Mohiuddin-Jacobs, S. J. L. Billinge, *J. Phys. Chem. A* **103**, 921 (1999).
14. G. H. Kwei, S. J. L. Billinge, S.-W. Cheong, J. G. Saxton, *Ferroelectrics* **164**, 57 (1995).
15. H. D. Rosenfeld, T. Egami, *Ferroelectrics* **164**, 133 (1995).
16. P. Debye, *Ann. Phys.-Berlin* **39**, 789 (1912).
17. P. Souvatzis, O. Eriksson, M. I. Katsnelson, S. P. Rudin, *Phys. Rev. Lett.* **100**, 095901 (2008).
18. A. F. Joffé, *Can. J. Phys.* **34**, (12A), 1342 (1956).
19. B. A. E. Yu, I. Ravich, I. A. Smirnov, *Semiconducting Lead Chalcogenides*, vol. 5 (Plenum, New York, 1970).
20. R. N. Tauber, A. A. Machonis, I. B. Cadoff, *J. Appl. Phys.* **37**, 4855 (1966).
21. T. M. Chuang *et al.*, *Science* **327**, 181 (2010).
22. S.J.B. and E.B. thank J. Richardson for his early support and enthusiasm for the project and dedicate the paper to him. We acknowledge useful discussions with A. Millis, P. Allen, R. Cohen, C. Farrow, and J. Hill. Work in the Billinge group was supported by the U.S. Department of Energy, Office of Basic Energy Sciences (DOE-BES), under contract DE-AC02-98CH10886. Work in the Kanatzidis group was supported by the Office of Naval Research. Work in the Spaldin group was supported by the NSF under award DMR-0940420. The neutron diffraction measurements were carried out at the Lujan Center at Los Alamos National Laboratory, and the x-ray experiments were carried out at the Advanced Photon Source, Argonne National Laboratory, both of which are supported by DOE-BES, and the calculations were performed at the San Diego Supercomputer Center, which is supported by NSF.

Supporting Online Material

www.sciencemag.org/cgi/content/full/330/6011/1660/DC1
Materials and Methods
SOM Text
Figs. S1 to S4
References

24 May 2010; accepted 16 November 2010
10.1126/science.1192759

Large Variations in Southern Hemisphere Biomass Burning During the Last 650 Years

Z. Wang,[1] J. Chappellaz,[2] K. Park,[1] J. E. Mak[1]*

We present a 650-year Antarctic ice core record of concentration and isotopic ratios ($\delta^{13}C$ and $\delta^{18}O$) of atmospheric carbon monoxide. Concentrations decreased by ~25% (14 parts per billion by volume) from the mid-1300s to the 1600s then recovered completely by the late 1800s. $\delta^{13}C$ and $\delta^{18}O$ decreased by about 2 and 4 per mil (‰), respectively, from the mid-1300s to the 1600s then increased by about 2.5 and 4‰ by the late 1800s. These observations and isotope mass balance model results imply that large variations in the degree of biomass burning in the Southern Hemisphere occurred during the last 650 years, with a decrease by about 50% in the 1600s, an increase of about 100% by the late 1800s, and another decrease by about 70% from the late 1800s to present day.

Carbon monoxide (CO) plays a key role in the chemistry of the troposphere, largely determining the oxidation potential of the atmosphere through its interaction with hydroxyl radical (OH). CO also interacts with atmospheric methane, a gas whose preindustrial variability is the topic of continuing debate (*1*, *2*). Little is known about the variability of CO before the industrial age (*3*) or about the anthropogenic impact on its budget, although both affect atmospheric CH_4 and O_3 budgets and related climate-chemistry interactions.

The main sources of atmospheric CO include atmospheric oxidation of methane and nonmethane hydrocarbons (NMHCs), biomass burning, and fossil fuel combustion (*4*). These sources account for about 90% of today's global CO budget (*4*). Stable isotopic ratios ($\delta^{13}C$ and $\delta^{18}O$) in atmospheric CO help to resolve the relative contributions of these sources and thus to better estimate the global CO budget (*5*). To date, no isotopic ratios from CO in ice have been reported, and few CO mixing ratio measurements have been reported (*1*, *3*, *6*). Through use of a recently developed analytical technique (*7*), we present measurements of CO concentration ([CO]), $\delta^{13}C$, and $\delta^{18}O$ from a South Pole ice core [89°57'S 17°36'W; 2800 m above sea level (asl)] and from the D47 ice core (67°23'S 154°03'E; 1550 m asl) in Antarctica (Fig. 1).

The combined changes in [CO], $\delta^{13}C$, and $\delta^{18}O$ during the past 650 years should reflect variations in both total CO flux and a shift in relative source strengths over time. [CO] shows a decreasing trend from 53 ± 5 parts per billion by volume (ppbv) in the mid-1300s to a minimum of 38 ± 5 ppbv in the 1600s. CO mixing ratio then increases to a relatively constant value of 55 ± 5 ppbv in the late 1800s. Good agreement was observed between our [CO] data and previous measurements on Antarctic ice samples (*3*, *6*). Trends in both $\delta^{13}C$ and $\delta^{18}O$ look similar to the [CO] record up to the late 1800s. $\delta^{13}C$ [Vienna Pee Dee belemnite (VPDB)] and $\delta^{18}O$ [Vienna standard mean ocean water (VSMOW)], respectively, decreased from –28.0 ± 0.3‰ and 0.6 ± 0.7‰ in the mid-1300s to –30.2 ± 0.3‰ and –3.4 ± 0.7‰ in the 1600s, then increased to –27.4 ± 0.3‰ and 0.8 ± 0.7‰ by the late 1800s. Minimum values of [CO], $\delta^{13}C$, and $\delta^{18}O$ roughly coincide with the Little Ice Age (LIA; circa 1500–1800), as defined in the Northern Hemisphere.

Observations from Berkner Island (79°32.90'S 45°40.7'W; 890 m asl) firn and present day samples are also shown in Fig. 1. The slight decrease of [CO] from the late 1800s to present day is thus accompanied by large shifts in both $\delta^{13}C$ and $\delta^{18}O$, which is a result of variations in relative source strengths during the past century. In particular, methane-derived CO, which is dependent upon methane concentration and depleted in both $\delta^{13}C$ and $\delta^{18}O$, increased dramatically—by 13 ppbv—during this time (Fig. 2). Because there was little difference in overall [CO] between the late 1800s and present day, contributions from other CO sources must have decreased by a similar amount. Data from Berkner Island firn air show an increase in [CO] and a decrease in $\delta^{13}C$ since 1970 (*8*), reflecting the increase in atmospheric methane (*9*).

The contribution from fossil fuel combustion is negligible before the 1900s according to historic CO_2 emissions data (*10*). In addition, simulations from the Model for Ozone and Related chemical Tracers (MOZART-4) (*11*) show the fossil fuel combustion contribution to today's CO budget in Antarctica is only 2 to 3 ppbv. Thus, the main sources of CO able to explain our signals are biomass burning and NMHC oxidation.

We can use isotopic compositions to help distinguish combustion-derived CO (such as biomass burning) from noncombustion-derived CO (such as hydrocarbon oxidation). $C^{18}O$ is a useful tracer for this because of large differences in the oxygen isotopic composition between combustion and noncombustion sources of CO (*12*). The $\delta^{18}O$ signature from combustion sources is significantly enriched as compared with the $\delta^{18}O$ signature from hydrocarbon oxidation processes (*12*, *13*). The $\delta^{18}O$ value for biomass burning–derived CO is generally between 15 and 22‰, depending on specific combustion conditions (*13*–*15*).

We used an isotope mass balance model to estimate the ratio of combustion to noncombustion

[1]Institute for Terrestrial and Planetary Atmospheres/School of Marine and Atmospheric Sciences, Stony Brook University, Stony Brook, NY 11794–5000, USA. [2]Laboratoire de Glaciologie et Géophysique de l'Environnement (LGGE), CNRS, University of Grenoble, BP 96, 38402 St. Martin d'Hères Cedex, France.

*To whom correspondence should be addressed. E-mail: john.mak@stonybrook.edu

sources over the time period of interest (*11*). Steady-state atmospheric conditions were assumed on the basis of the relatively short lifetime of CO (weeks to months) as compared with the integrated sampling time for a typical ice core sample (~10 years for the D47 ice core and ~30 years for the South Pole ice core). Resulting source emission estimates are shown in Fig. 2. Also shown are source emission estimates over the last three decades and those in present day. CO from NMHC oxidation did not change significantly, whereas CO from biomass burning showed a large "saddle" trend, with maxima in both the mid-1300s and the late 1800s and a minimum in the 1600s. The observed trend in [CO], $\delta^{13}C$, and $\delta^{18}O$ was therefore mostly driven by variations in biomass burning, and compared with present day, biomass burning was almost the same in the late 1800s as that in the mid-1300s. This is consistent with the correlation observed between $\delta^{18}O$ and CO concentration (fig. S1). The *y* intercept of 9‰, corrected for the inverse mass-dependent kinetic isotope effect (KIE) for CO+OH (*16*) during atmospheric transport, leads to a mean oxygen isotopic signature of the source of 15 to 18‰, which indicates a predominant combustion source.

We have assumed that the observations were driven by variations in CO source strengths. It is possible, however, that the removal rate of CO by OH could have changed. However, if that were the case, then a slight enrichment in $\delta^{13}C$ should be observed because of the KIE (*16*). This is contrary to the observations. The second largest loss mechanism known for CO (but only accounting for 10%) is uptake by soils, which is largely dependent on soil surface area and mean temperature (*17*), both of which have not changed much in the Southern Hemisphere during the past several hundred years (*18*).

Satellite data combined with biogeochemical models to interpret the interannual variability of global biomass burning emissions show that from 1997 to 2004, lower temperature and higher precipitation correlated with reduced biomass burning emission (*19*). On longer time scales, biomass burning was shown to increase with the rapid Dansgaard/Oeschger warmings of the last glacial, probably because of increased vegetation productivity and fuel availability for burning (*20*).

Our calculated biomass burning trend (Fig. 2) is generally consistent with the tropical charcoal index (Fig. 3) (*21*). The charcoal index, which is a proxy for biomass burning, suggests a decline from ~0 to ~1750 followed by a sharp increase between 1750 and 1870 and a substantial decrease during the past century (*21*). Because of the fast deposition of charcoal particles, the charcoal index reflects a more regional component of biomass burning as compared with CO; however, the general trends for the two records are consistent within the range of calculated uncertainty, with perhaps the exception of the period of 1600–1700. The initial decline in biomass burning occurred in concert with a global cooling trend, reflecting the impact of climate change (*21*). The cooling was more muted on average in the Southern Hemisphere (*22*). But in a region such as southern South America, warm episodes are recorded before 1350 and in the early 19th century (*23*), coinciding with the stronger biomass burning emissions of CO deduced from our record. Since the 1700s, the increase of biomass burning has probably been influenced by both natural and anthropogenic forcings. This trend is also consistent with Berkner Island firn air data from ~1970 to present day. Such a reduction may result from a shift toward intensive grazing and fire management (*24*), which could lead to a change in landscape makeup and subsequently less biomass availability in some regions (*25*).

Biomass burning changes during the last two millennia have also been evaluated by using $[CH_4]$ and $\delta^{13}CH_4$ records from the Law Dome ice core (*1*). These investigators conclude that the pyrogenic emissions of CH_4 decreased by ~40% on the

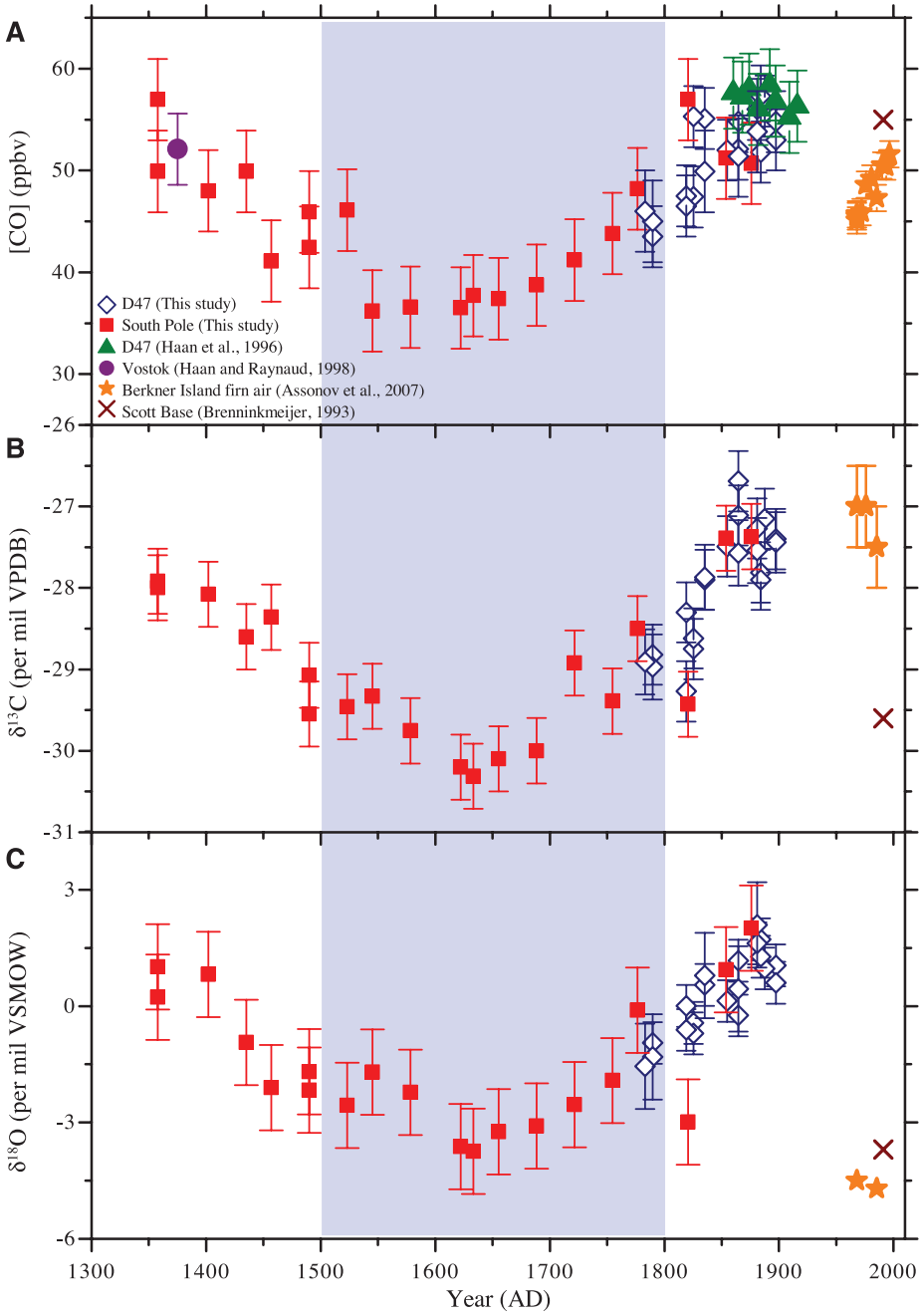

Fig. 1. The 650-year records of [CO], $\delta^{13}C$, and $\delta^{18}O$ from two ice cores: D47 ice core (diamonds) and South Pole ice core (squares). (**A**) [CO]. (**B**) $\delta^{13}C$. (**C**) $\delta^{18}O$. Error bars represent analytical uncertainties. The shaded area shows the timing of the LIA. Also shown are observations of annually averaged [CO], $\delta^{13}C$, and $\delta^{18}O$ of atmospheric CO (crosses) at Scott Base in 1991 (*13*). Berkner Island firn air data (stars) (*8*) roughly covering the last three decades of the 20th century show a 5 ppbv increase of [CO], 2.5‰ decrease of $\delta^{13}C$, and a slight increase in $\delta^{18}O$ since the late 1960s.

global scale in 1700 relative to the emissions from 0 to 1000, a figure that is consistent with our calculated ~50% drop of biomass burning emissions of CO during the 1600s in the Southern Hemisphere. Furthermore, recent research based on the stable isotopic ratios of methane in the West Antarctic Ice Sheet (WAIS) Divide ice core (79°27.7'S 112°7.51'W; 1759 m asl) also indicates that the median biomass burning source strength decreased by 38 ± 1% from the period of 990–1460 to 1689–1730 (*26*).

Long-term variations in atmospheric circulation could have partly modulated the long-range transport of biomass burning CO from the tropics to the high-latitude Southern Hemisphere (*27*), thus contributing in part to the calculated CO variability. For instance, a strengthened polar vortex could inhibit latitudinal exchanges and extratropical CO intrusion into the Antarctic atmosphere. However, the last period of intensification of southern circumpolar westerlies and accompanying relatively cooler conditions over East Antarctica (*28*) and West Antarctica occurred ~1200 to 1000 years ago (*29*), well before the period of this study. Although it cannot be entirely ruled out, indications are that circumpolar circulation did not change significantly during this period and did not have a large impact on CO large-scale transport.

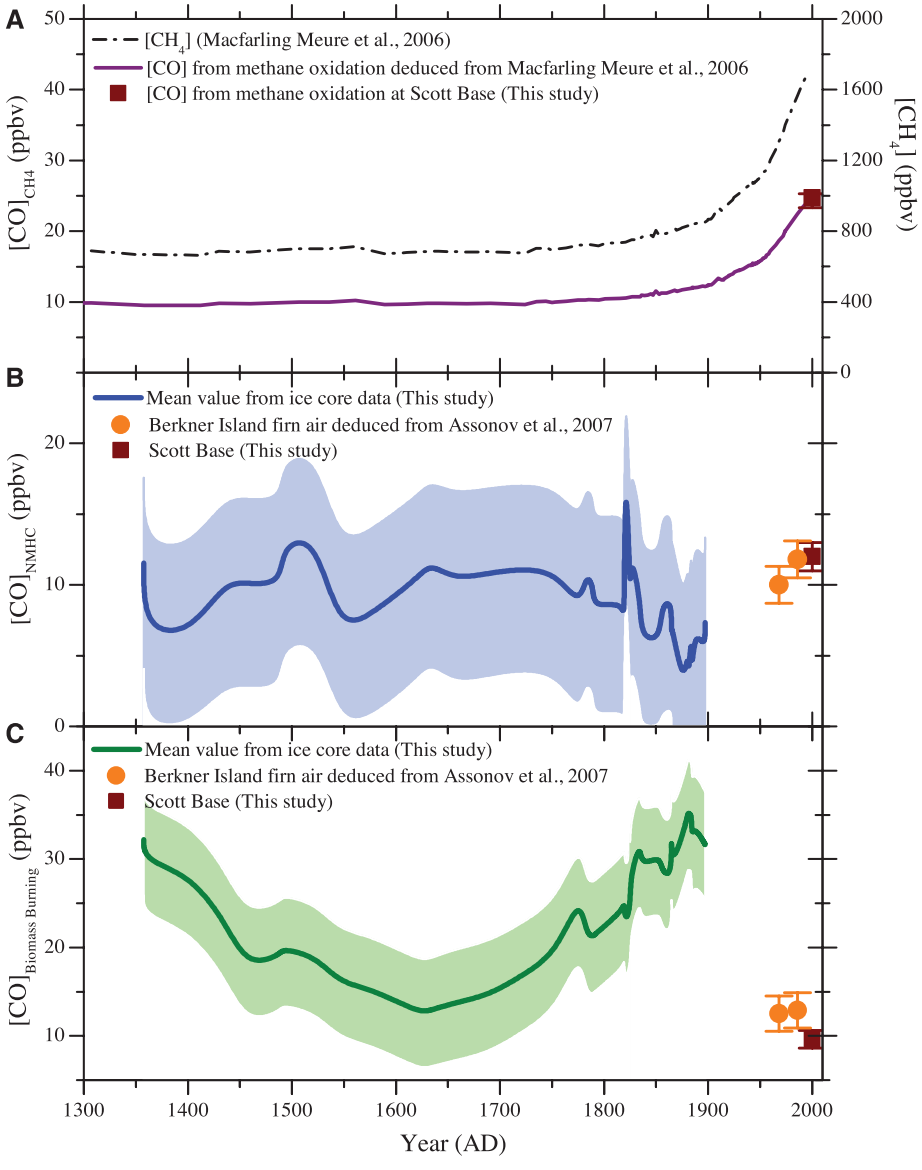

Fig. 2. Modeled CO source partitioning based on observations and an isotope mass balance model. (**A**) [CO] from methane oxidation. (**B**) [CO] from NMHC oxidation. (**C**) [CO] from biomass burning. Different scenarios have been tested in the model to show the sensitivity of minor sources (*11*). Thick lines in (B) and (C) represent the mean values of different scenarios, and shaded areas represent different scenario run results and uncertainties. [CH_4] data are from the Law Dome record (*9*). [CO] derived from the three major sources since the late 1960s was calculated based on Berkner Island firn air data (*8*) and an isotope mass balance model (orange circles). CO source partitioning at present day was calculated based on MOZART-4 simulation and CO measurements (annually averaged, 1997–2004) at Scott Base (red squares).

Another possible process that has a major effect on the meridional transport of CO is the movement of the Intertropical Convergence Zone (ITCZ) (*30*). Paleoclimatic evidence from continental Asia (*31*), Africa (*32*), the Americas (*33*), and the Pacific Ocean (*34*) suggests that a southward shift of the ITCZ occurred during the past millennium, reaching its southernmost position some time during the LIA (*34*). As the ITCZ shifts southward, less CO produced from biomass burning will be transported to the Southern Hemisphere. This would have reduced the contribution of Southern Hemisphere biomass burning to [CO] observed in Antarctica during the LIA. A southward shift of the ITCZ position would also shift rainfall patterns southward because precipitation follows the ITCZ (*35*). A southward shift of precipitation could also contribute to a decrease in biomass burning during the LIA because dry conditions favor biomass burning.

Previous modeling studies suggest that preindustrial biomass burning was much lower than today, with a reduction of up to 90% (*36*–*38*). This is the common assumption in climate model simulations. However, our results show that present-day CO from Southern Hemisphere biomass burning is lower than at any other time during the last 650 years. This is particularly relevant because assumptions on preindustrial [CO] are an important component for correctly estimating the radiative forcing of tropospheric ozone in preindustrial times (*39*). [CO] changes due to biomass burning also suggest that there were decadal and centennial scale variations in average concentrations of black carbon, which is another major atmospheric constituent produced with burning, leading to the unanswered question of its potential role in long-term climate variability.

References and Notes

1. D. F. Ferretti *et al.*, *Science* **309**, 1714 (2005).
2. J. R. Petit *et al.*, *Nature* **399**, 429 (1999).
3. D. Haan, P. Martinerie, D. Raynaud, *Geophys. Res. Lett.* **23**, 2235 (1996).
4. W. Seiler, *Tellus* **26**, 116 (1974).
5. P. Bergamaschi, R. Hein, C. A. M. Brenninkmeijer, P. J. Crutzen, *J. Geophys. Res.* **105** (D2), 1929 (2000).
6. D. Haan, D. Raynaud, *Tellus* **50**, 253 (1998).
7. Z. Wang, J. E. Mak, *Atmos. Meas. Tech.* **3**, 1307 (2010).
8. S. S. Assonov *et al.*, *Atmos. Chem. Phys.* **7**, 295 (2007).
9. C. M. Macfarling Meure *et al.*, *Geophys. Res. Lett.* **33**, L14810 (2006).
10. G. Marland, T. A. Boden, R. J. Andres, "Global, Regional, and National Fossil-Fuel CO_2 Emissions," in *Trends: A Compendium of Data on Global Change* (Carbon Dioxide Information Analysis Center, Oak Ridge National Laboratory, U.S. Department of Energy, Oak Ridge, TN, 2008).
11. Materials and methods are available as supporting material on *Science* Online.
12. C. A. M. Brenninkmeijer, T. Rockmann, *J. Geophys. Res.* **102** (D21), 25477 (1997).
13. C. A. M. Brenninkmeijer, *J. Geophys. Res.* **98**, 10595 (1993).
14. S. Kato, H. Akimoto, T. Rockmann, M. Braunlich, C. A. M. Brenninkmeijer, *Atmos. Environ.* **33**, 4357 (1999).
15. C. M. Stevens, A. F. Wagner, *Z. Naturforsch. A* **44**, 376 (1989).
16. C. M. Stevens *et al.*, *Int. J. Chem. Kinet.* **12**, 935 (1980).
17. R. E. Inman, R. B. Ingersoll, E. A. Levy, *Science* **172**, 1229 (1971).

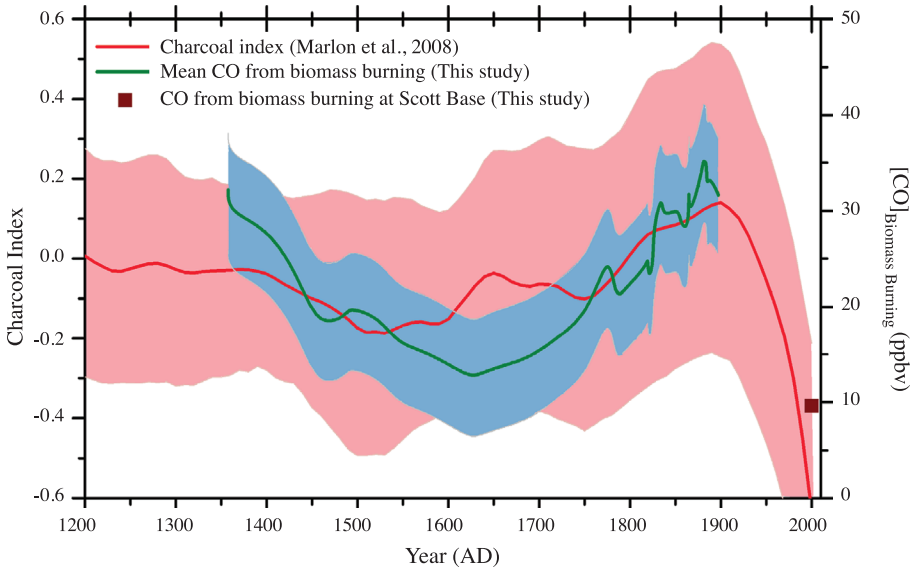

Fig. 3. Correlation between the derived CO from biomass burning (green line) and the sedimentary charcoal record compilation in the tropics (30°N–20°S) (red line) (*21*). The red shaded area represents charcoal index measurement uncertainties. The blue shaded area is the same as that in Fig. 2C. Also shown is the MOZART-4–simulated CO from biomass burning emission at Scott Base for the modern atmosphere.

18. M. E. Mann, P. D. Jones, *Geophys. Res. Lett.* **30**, 1820 (2003).
19. G. R. van der Werf *et al.*, *Atmos. Chem. Phys.* **6**, 3423 (2006).
20. A.-L. Daniau, S. P. Harrison, P. J. Bartlein, *Quat. Sci. Rev.* **29**, 2918 (2010).
21. J. R. Marlon *et al.*, *Nat. Geosci.* **1**, 697 (2008).
22. M. E. Mann *et al.*, *Science* **326**, 1256 (2009).
23. R. Neukom *et al.*, *Clim. Dyn.* (2010).
24. K. K. Goldewijk, *Global Biogeochem. Cycles* **15**, 417 (2001).
25. S. J. Pyne, *World Fire: The Culture of Fire on Earth* (Univ. of Washington Press, Seattle, 1995).
26. J. A. Mischler *et al.*, *Global Biogeochem. Cycles* **23**, Gb4024 (2009).
27. D. P. Edwards *et al.*, *J. Geophys. Res.* **111** (D14), D14312 (2006).
28. V. Masson *et al.*, *Quat. Res.* **54**, 348 (2000).
29. P. A. Mayewski *et al.*, *Rev. Geophys.* **47**, RG1003 (2009).
30. W. Seiler, H. Giehl, E. G. Brunke, E. Halliday, *Tellus* **36**, 219 (1984).
31. D. M. Anderson, J. T. Overpeck, A. K. Gupta, *Science* **297**, 596 (2002).
32. D. Verschuren, K. R. Laird, B. F. Cumming, *Nature* **403**, 410 (2000).
33. G. H. Haug, K. A. Hughen, D. M. Sigman, L. C. Peterson, U. Röhl, *Science* **293**, 1304 (2001).
34. J. P. Sachs *et al.*, *Nat. Geosci.* **2**, 519 (2009).
35. J. C. Stager, C. Cocquyt, R. Bonnefille, C. Weyhenmeyer, N. Bowerman, *Quat. Res.* **72**, 47 (2009).
36. P. J. Crutzen, P. H. Zimmermann, *Tellus* **43**, 136 (1991).
37. A. Ito, J. E. Penner, *Global Biogeochem. Cycles* **19**, GB2028 (2005).
38. F. Mouillot, A. Narasimha, Y. Balkanski, J. F. Lamarque, C. B. Field, *Geophys. Res. Lett.* **33**, L01801 (2006).
39. M. Gauss *et al.*, *Atmos. Chem. Phys.* **6**, 575 (2006).

40. We thank C. A. M. Brenninkmeijer for useful help and discussions. South Pole ice core samples were provided by the National Ice Core Laboratory (NICL) and drilled by J. Cole-Dai and colleagues. We greatly thank M. Twickler for ice allocation and thank B. Bencivengo, E. Cravens, and G. Hargreaves for cutting and shipping ice. We thank the drillers (LGGE) and logistics (French polar institute) who made D47 drilling possible. We also thank E. Brook and J. E. Lee from Oregon State University for providing bubble-free ice and M. Montagnat, LGGE, CNRS for providing monocrystalline and polycrystalline bubble-free ice. We also thank L. Emmons for useful help on MOZART-4 simulation and NCAR for providing a supercomputing environment for MOZART-4 simulation. Z.W. strongly thanks P. Martinerie for logistical support in Grenoble. We are grateful to M. Zhang, D. Black, V. Masson-Delmotte, and D. Knopf for their useful comments. We thank A. Matthews from Mt. Sinai High School for providing a walk-in freezer in which to prepare some ice core samples. This work was supported by NSF grant OCE0731406, the European Science Foundation (ESF) EURO-CORES Programme EuroCLIMATE (contract ERAS-CT-2003-980409 of the European Commission, DG Research, FP6), Institut National des Sciences de l'Univers (INSU) project ISOTRACE-FP21, and the French ANR NEEM (ANR-O7-VULN-09-001).

Supporting Online Material

www.sciencemag.org/cgi/content/full/science.1197257/DC1
Materials and Methods
Figs. S1 to S4
Tables S1 to S3
References

1 September 2010; accepted 1 November 2010
Published online 2 December 2010;
10.1126/science.1197257

Structural Basis of Biological N_2O Generation by Bacterial Nitric Oxide Reductase

Tomoya Hino,[1,2,3] Yushi Matsumoto,[1,4] Shingo Nagano,[1,5] Hiroshi Sugimoto,[1] Yoshihiro Fukumori,[6] Takeshi Murata,[2,3] So Iwata,[2,3,7] Yoshitsugu Shiro[1]

Nitric oxide reductase (NOR) is an iron-containing enzyme that catalyzes the reduction of nitric oxide (NO) to generate a major greenhouse gas, nitrous oxide (N_2O). Here, we report the crystal structure of NOR from *Pseudomonas aeruginosa* at 2.7 angstrom resolution. The structure reveals details of the catalytic binuclear center. The non-heme iron (Fe_B) is coordinated by three His and one Glu ligands, but a His-Tyr covalent linkage common in cytochrome oxidases (COX) is absent. This structural characteristic is crucial for NOR reaction. Although the overall structure of NOR is closely related to COX, neither the D- nor K-proton pathway, which connect the COX active center to the intracellular space, was observed. Protons required for the NOR reaction are probably provided from the extracellular side.

Nitrous oxide gas (N_2O) is now the greatest threat to the ozone layer and also induces climate change as a greenhouse gas more powerful than carbon dioxide and methane (*1*). Agricultural fertilizers, fossil fuel combustion, biomass burning, and animal waste contribute to N_2O production. However, the largest emission source of N_2O into the atmosphere is bacterial breakdown of nitrogen compounds in soils and in the oceans. Denitrifiers perform the step-by-step chemical reduction of nitrogen oxides (NO_3^- and NO_2^-) to N_2, producing N_2O as an intermediate by-product: $NO_3^- \rightarrow NO_2^- \rightarrow NO \rightarrow N_2O \rightarrow N_2$. The key enzyme in N_2O production is nitric oxide reductase (NOR), which catalyzes the reduction of nitric oxide (NO) with two electrons and two protons: $2NO + 2e^- + 2H^+ \rightarrow N_2O + H_2O$. The NOR reaction is also of interest to synthetic chemists because it involves N-O bond cleavage and N-N bond formation (Scheme 1). Structural and functional models of the active site of NOR have been syn-

[1]RIKEN SPring-8 Center, 1-1-1 Kouto, Sayo, Hyogo 679-5148, Japan. [2]Japan Science and Technology Agency, Exploratory Research for Advanced Technology, Human Receptor Crystallography Project, Yoshida-Konoe-cho, Sakyo-ku, Kyoto 606-8501, Japan. [3]Department of Cell Biology, Graduate School of Medicine, Kyoto University, Yoshida-Konoe-cho, Sakyo, Kyoto 606-8501, Japan. [4]Division of Protein Chemistry, Post-Genome Science Center, Medical Institute of Bioregulation, Kyushu University, Fukuoka 812-8552, Japan. [5]Department of Chemistry and Biotechnology, Graduate School of Engineering, Tottori University, Tottori 680-8552, Japan. [6]Graduate School of Natural Science and Technology, Kanazawa University, Kanazawa, Ishikawa 920-1192, Japan. [7]Division of Molecular Bioscience, Membrane Protein Crystallography Group, Imperial College London, Exhibition Road, London SW7 2AZ, UK.